e-*Blood*

Engineered cell homing

Debanjan Sarkar,[1] Joel A. Spencer,[2,3] Joseph A. Phillips,[1] Weian Zhao,[1] Sebastian Schafer,[1] Dawn P. Spelke,[1] Luke J. Mortensen,[2] Juan P. Ruiz,[1] Praveen Kumar Vemula,[1] Rukmani Sridharan,[1] Sriram Kumar,[1] Rohit Karnik,[4] Charles P. Lin,[2] and Jeffrey M. Karp[1]

[1]Center for Regenerative Therapeutics and Department of Medicine, Brigham & Women's Hospital, Harvard Medical School, Harvard Stem Cell Institute, Harvard–Massachusetts Institute of Technology Division of Health Sciences and Technology, Cambridge, MA; [2]Center for Systems Biology, Advanced Microscopy Program, Wellman Center for Photomedicine, Massachusetts General Hospital, Harvard Medical School, Boston, MA; [3]Department of Biomedical Engineering, Science and Technology Center, Tufts University, Medford, MA; and [4]Department of Mechanical Engineering, Massachusetts Institute of Technology, Cambridge, MA

One of the greatest challenges in cell therapy is to minimally invasively deliver a large quantity of viable cells to a tissue of interest with high engraftment efficiency. Low and inefficient homing of systemically delivered mesenchymal stem cells (MSCs), for example, is thought to be a major limitation of existing MSC-based therapeutic approaches, caused predominantly by inadequate expression of cell surface adhesion receptors. Using a platform approach that preserves the MSC phenotype and does not require genetic manipulation, we modified the surface of MSCs with a nanometer-scale polymer construct containing sialyl Lewis^x (sLe^x) that is found on the surface of leukocytes and mediates cell rolling within inflamed tissue. The sLe^x engineered MSCs exhibited a robust rolling response on inflamed endothelium in vivo and homed to inflamed tissue with higher efficiency compared with native MSCs. The modular approach described herein offers a simple method to potentially target any cell type to specific tissues via the circulation. (*Blood*. 2011;118(25):e184-e191)

Introduction

Cell therapy offers enormous hope for solving some of the most tragic illnesses, diseases, and tissue defects; however, a significant barrier to the effective implementation of cell therapies is the inability to target a large quantity of viable cells with high efficiency to tissues of interest. Systemic infusion is desired because it minimizes the invasiveness of cell therapy and maximizes practical aspects of repeated doses. Systemic infusion also permits the cells to mimic natural cell trafficking processes and helps to ensure that cells remain in close proximity to oxygen and nutrient-rich blood vessels. Mesenchymal stem cells (MSCs) represent a potent source of immunoprivileged postnatal cells that are conveniently isolated autologously or used from an allogeneic source without the addition of an immunosuppressive regimen, and are currently being investigated in more than 100 clinical trials,[1] the majority of which use a systemic route of delivery. Although they exhibit favorable therapeutic properties, including the capacity for multilineage differentiation followed by production of a specific extracellular matrix (eg, bone, cartilage, or fat)[2,3] and they exhibit immunomodulatory potential to reduce inflammation through secretion of soluble paracrine or endocrine factors,[4] typically less than 1% of the infused MSCs reach the target tissue.[5,6] The inefficient MSC homing is the result of a variety of factors but is typically attributed to an absence of relevant cell surface homing ligands.[7,8] Specifically, culture expanded MSCs develop heterogeneous receptor expression and lose key homing ligands during cell culture,[9] which contributes to the inefficiency of in vivo MSC homing. This represents a major challenge for minimally invasive MSC-based therapies that require a high efficiency of engraftment within specific tissues.[10] Thus, it can be rationalized that engineering the surface of cells, such as MSCs, with adhesion ligands can enhance the homing of cells to specific tissues after systemic infusion.

The first step of leukocyte extravasation involves capture of leukocytes flowing freely in the bloodstream, mediated by glycoproteins known as selectins. P- and E-selectins are highly expressed by the vascular endothelium locally within inflamed tissue and are the principal mediators for initial rolling response for the homing of leukocytes to sites of inflammation.[11,12] Selectins also mediate hematopoietic stem cell rolling within the bone marrow.[13] These interactions are transient in nature, being characterized by rapid on rates and force-sensitive off rates, which results in a slow rolling motion of the leukocytes along the vascular endothelium and are typically mediated by selectins that recognize ligands containing carbohydrate moieties of the sialyl Lewis^x (sLe^x) family.[12,14] sLe^x is the active site of P-selectin glycoprotein ligand 1 (PSGL-1), which is expressed by hematopoietic stem cells and leukocytes. This rolling response is critical for enabling chemokine signaling and arrest by integrins, which eventually results in extravasation; indeed, in vitro and in vivo studies have demonstrated that cell rolling is prerequisite for firm adhesion of leukocytes, and abrogation of the rolling response leads to decreased firm adhesion.[11,12,15,16] This indicates the importance of cell rolling as a crucial step for cell homing. Thus, inducing an MSC rolling response may be expected to enhance their homing ability and increase the engraftment efficiency after systemic delivery. The proof of principle for this hypothesis is provided by approaches that

Submitted October 4, 2010; accepted September 30, 2011. Prepublished online as *Blood* First Edition paper, October 27, 2011; DOI 10.1182/blood-2010-10-311464.

This article contains a data supplement.

The publication costs of this article were defrayed in part by page charge payment. Therefore, and solely to indicate this fact, this article is hereby marked "advertisement" in accordance with 18 USC section 1734.

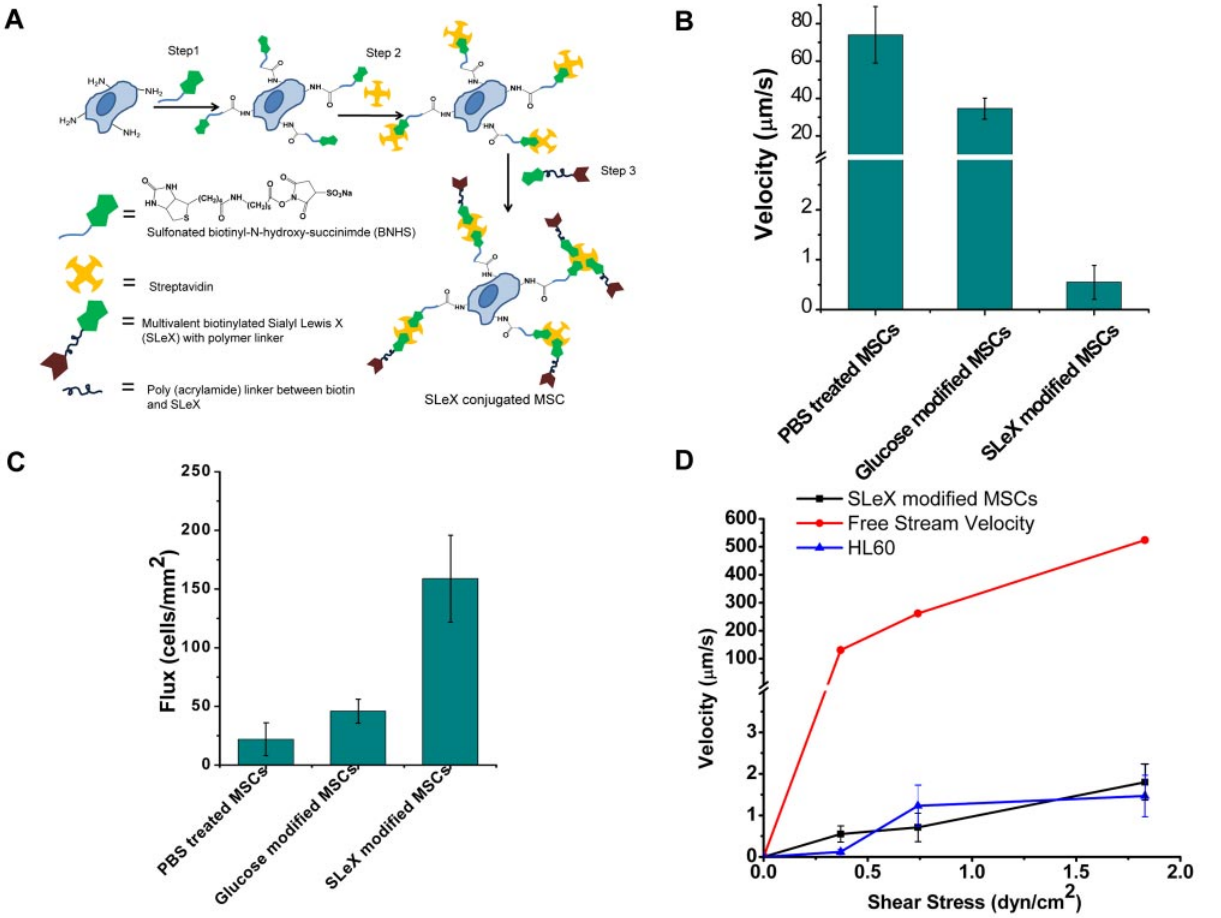

Figure 1. Cell surface engineered MSCs display enhanced rolling intactions in vitro. (A) Conjugation of sLe^x on the surface of the MSCs through covalent biotinylation and a streptavidin-biotin bridge. (B) Velocity of sLe^x-modified cells compared with PBS-treated cells and glucose-modified cells at 0.36 dyne/cm^2 on P-selectin–coated substrates. (C) Number of interacting sLe^x-modified cells compared with PBS-treated cells and glucose-modified cells per unit area at 0.36 dyne/cm^2 on P-selectin–coated substrate over 10 seconds with 0.45 mm^2 area. (D) Velocity of sLe^x-modified MSCs, HL60, and free stream velocity (theoretically calculated from flow chamber geometry and fluid flow rate) at increasing shear stress.

have involved enzymatic and genetic modification of MSCs to alter the repertoire of cell surface markers.[7,17] Although these strategies can improve the delivery of MSCs to sites of inflammation, the broad applicability of these technologies is limited. Enzymatic modification is complex and limited to modification of existing cell surface receptors, whereas genetic manipulation of cells may not be practical for altering the expression of more than a single receptor, and presents potential safety concerns. Recently, we demonstrated simple, platform strategies to conjugate sLe^x, a ligand that interacts with selectins to promote cell rolling.[18,19] However, in vitro the sLe^x-modified MSCs were not able to roll on a P-selectin–coated surface beyond approximately 0.7 dyne/cm^2 shear stress, which represents a challenge to target these modified MSCs in vivo.

Here we present a strategy to promote a robust MSC rolling response that offers a simple method to potentially target any cell type to specific tissues via the circulation. Functionalization of MSCs with a high ligand density was achieved through systematic optimization of a new protocol to modify the cells in suspension with a nanometer-scale polymer construct containing sLe^x, which induced a robust rolling response both in vitro and in vivo. We demonstrate that this method enhances the ability of MSCs to home to inflamed tissues without compromising MSC proliferation, multilineage differentiation potential, and secretion of pertinent paracrine factors.

Methods

Materials

Primary human MSCs, isolated from human marrow of healthy consenting donors, were obtained from the Center for Gene Therapy at Tulane University (which has a grant from National Center for Research Resources of the National Institutes of Health, grant P40RR017447). P-selectin was purchased from R&D Systems, and multivalent biotinylated sialyl Lewis(x)–poly(acrylamide) (sialyl-Lewis^X-PAA-biotin [BsLe^x]) was purchased from Glycotech where sialyl-Lewis^X-PAA-biotin contains 4 sLe^x units. α-MEM, L-glutamine, and Penn-Strep were purchased from Invitrogen. Sulfonated biotinyl-*N*-hydroxy-succinimide (BNHS) was purchased from Thermo Fisher Scientific, and FBS was purchased from Atlanta Biologicals. Biotin-4-fluorescein was purchased from Invitrogen. Anti–human cutaneous lymphocyte antigen antibody (HECA-452), the secondary antibody (FITC mouse anti–rat IgM), FITC CD90, and PE-Cy5 antibody were purchased from BD Biosciences. FACS buffer is PBS with 1% FBS. All other chemicals and reagents were purchased from Sigma-Aldrich and were used without further purification unless specified.

Surface modification of MSCs with a rolling ligand

The conjugation of BsLe^x to the MSC surface through biotin-streptavidin was performed under optimized conditions (supplemental Figure 1, see the Supplemental Materials link at the top of the article) in PBS (pH 7.4, without Ca/Mg) at room temperature. Typically, media was aspirated from 80% to 90% confluent T75 flasks, and cells were trypsinized using 1 times trypsin-EDTA solution, centrifuged into a pellet, and washed with PBS twice. The resulting cell pellet was dispersed in sulfonated biotinyl-*N*-hydroxy-succinimide, BNHS solution (1mM, 1 mL), which was allowed to incubate for 10 minutes at room temperature (Reaction Step 1, Figure 1A). The cells were then pelleted and washed with PBS twice by centrifugation to remove unattached and/or physically adsorbed BNHS from the cell surface. Streptavidin solution (50 μg/mL in PBS, 1 mL) was then used to treat the cells for 1 minute at room temperature (Reaction Step 2, Figure 1A). The cells were then pelleted and washed with PBS. To the streptavidin-conjugated cells, BsLe^x solution (5 μg/mL in PBS, 1 mL) was added, and the suspension was allowed to incubate for 5 minutes at room temperature (Reaction Step 3, Figure 1A). Finally, the cells were pelleted and washed with PBS.

Preparation of P-selectin surfaces

The well surfaces within a 6-well plate were coated with P-selectin solution (5 μg/mL in PBS, 1 mL) for 18 hours on a plate shaker at room temperature. All P-selectin surfaces were freshly prepared before the flow chamber assay.

Flow chamber assay

For the analysis of cell velocities through the flow chamber, the cells were suspended in MSC expansion media ($\sim 1 \times 10^5$ cells/mL) for the flow chamber assay. A circular parallel plate flow chamber (Glycotech) with 127-μm gasket thickness and a width of 2.5 mm was used. To monitor cell rolling, phase-contrast microscopy (TE2000-U Inverted Nikon Microscope with a DS-Qi1 Monochrome Cooled Digital Camera) was used, and images were recorded in a 10 times field at 10-second intervals. The velocity of the cells was calculated by measuring the distance cells traveled within a 10-second interval. A cell was classified as rolling if it rolled for 10 seconds while remaining in the field of view and if it traveled at an average velocity less than 50% of the calculated free stream velocity of a noninteracting cell. The flux was calculated manually based on number of cells interacting with the substrate and remaining in the field view for 10 seconds. Both the firmly adhered cells and rolling cells were considered for the flux calculation. To assess the effect of shear rate, the rolling velocity and the flux were measured at shear stresses, including 0.36, 0.72, and 1.89 dyne/cm^2.

In vivo animal experiment

Dynamic real-time intravital confocal microscopy. Homing of unmodified and sLe^x-modified MSCs to the skin was imaged noninvasively (in real time) using a custom-built video-rate laser-scanning confocal microscope designed specifically for live animal imaging.[20] To image the vasculature and surrounding tissue, we positioned the mouse's ear on a coverslip (with index matching gels) and obtained high-resolution images with cellular details through the intact mouse skin at depths of up to 250 μm. The laser beams were focused onto the sample (mouse ear skin) using a 60×, 1.2NA water immersion objective lens (Olympus). DiD- and DiR-labeled MSCs were excited with a 635-nm continuous wave laser (Coherent) and detected through a 695-nm ± 27.5-nm band pass filter (Omega Optical) for DiD (red channel) and through a 770-nm-long pass filter (Omega Optical) for DiR (green channel). Because a large portion of DiD fluorescence leaks into the DiR channel and some DiR fluorescence leaks into the DiD channel, DiD$^+$ cells were identified as having a red-to-green ratio more than 1 (orange-red hue), whereas DiR$^+$ cells were identified as having a red-to-green ratio less than 1 (yellow-green hue). FITC-dextran (blue channel) was excited with a 491-nm continuous wave laser (Cobalt) and detected through a 520-nm ± 20-nm bandpass filter (Semrock). Video-rate movies were recorded for analysis of cell rolling. Because this system operates at 30 frames per second, the live video was recorded to measure the velocities of rolling cells. In the case of static images, 15 to 30 frames were averaged from the live video mode to improve the signal-to-noise ratio. However, instead of recording single images, we recorded z-stacks to quantify the number of cells that transmigrated the blood vessels. We computed the average rolling velocity (using ImageJ Version 1.45a software, National Institutes of Health) as the displacement of the centroid of the cell divided by the time interval between observations. The total number of "homed" cells from each MSC population and the percentage of MSCs in each population that had transmigrated the blood vessel endothelium within the mouse ear were quantified from the z-stacks acquired. For publication purposes, the contrast and brightness of the images were changed using ImageJ Version 1.45a software.

Expression of P-selectin and E-selectin. Anti–P-selectin (CD62P), anti–E-selectin (CD62E), and IgG1λ were purchased from BD Biosciences and labeled with Cy5 or Cy3 monoreactive dyes according to the manufacturer's protocol (GE Healthcare). Antibody conjugates were diluted into sterile saline to a final concentration of 0.1 mg/mL. A total of 100 μL of antibody solution was administered via tail vein injection 20 hours after lipopolysaccharide (LPS) injection. Cy5 was excited using 633 nm, and emission was detected between 667 nm and 722 nm. Cy3 was excited using 532 nm, and emission was detected between 573 nm and 613 nm. Adjacent z-stack images with 10-μm step size were acquired along a vein 24 hours after LPS injection. Maximum intensity projections of the z-stacks were created using ImageJ Version 1.45a software and then manually stitched together in Photoshop CS2 to create a map of the vessel.

In vivo blocking of P-selectin. A total of 100 μg/20 g unlabeled anti–P-selectin (BD Biosciences PharMingen, NA/LE rat anti–mouse 553741) or IgG1λ isotype (BD Biosciences PharMingen, NA/LE rat anti–mouse 559157) was mixed with MSC and injected retro-orbitally 24 hours after LPS injection. Homing was assessed 24 hours after MSC injections as described previously.

Calculation of in vivo cell velocities and hemodynamic parameters. The velocity of the fastest moving cells was used as an estimate of the maximal cell velocity (V_{max}), and the mean blood flow velocity (V_{mean}) was calculated, assuming Newtonian flow, from the maximal cell velocity and the ratio of cell diameter to vessel diameter, as $V_{max}/(2 - \epsilon^2)$, where ϵ = cell diameter/vessel diameter. Cells with velocity greater than the mean blood flow velocity were not considered for analysis of rolling interactions. Critical velocity (V_{crit}), which represents the lowest velocity at which a cell traveling close to the vessel wall can move without receptor/ligand-mediated adhesive interactions, was calculated as $V_{mean}\epsilon(2 - \epsilon)$.[21,22] All labeled cells moving above V_{crit} were considered noninteracting, whereas cells moving below V_{crit} were engaged in adhesive interactions with the vessel wall and were considered rolling. Venular wall shear rate (γ) was calculated, assuming Newtonian flow: 4.9 (8 V_{mean}/d), where V_{mean} is the mean blood flow velocity and d the diameter of the vessel. The constant 4.9 is a mean empirical correction factor obtained from recently described velocity profiles measured in microvessels in vivo.[23,24] The venular wall shear stress(τ) was $\gamma \times$ blood viscosity (η), where η was assumed to be 0.025 poise.[25]

Statistical analysis

For multiple pairwise comparisons, a 2-tailed Student *t* test was used with the Bonferroni correction. Two-way ANOVA was used to assess statistical significance of cell preparations performed on different days and isotype versus antibody blocking for in vivo antibody blocking experiments. Error bars in graphs represent SDs.

Results and discussion

Surface modification of MSCs with a rolling ligand, sLe^x

Given that culture-expanded MSCs do not express PSGL-1,[7] we chemically immobilized sLe^x on the MSC surface to investigate the targeting of systemically administered MSCs to sites of inflammation. We used a 3-step modification to immobilize sLe^x that involves

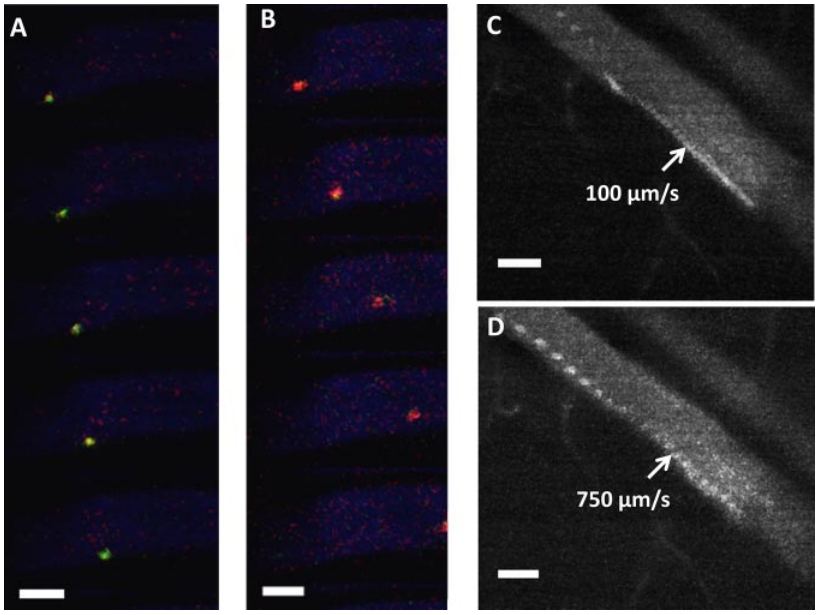

Figure 2. In vivo rolling of surface engineered MSCs. (A) In vivo confocal video images of sLe^x-MSCs with velocity 250 μm/s (green) were taken at 30 frames/s within the inflamed ear vessel (blue) after injection of MSCs. (B) In vivo confocal video images of unmodified MSCs with velocity 1100 μm/s (red) were taken at 30 frames/s within the inflamed ear vessel (blue) after injection of MSCs. (A-B) The vessel diameter is approximately 60 μm, and the critical velocity is 571 μm/s. (C) Representative image of sLe^x-MSCs interacting with inflamed endothelium in approximately 60 μm vessel resulting in velocity of 100 μm/s (103 frames stacked with 30 fps; ie, sLe^x-MSC remains in the field of view for $>$ 3.3 seconds). (D) Representative image of unmodified MSCs interacting with inflamed endothelium in approximately 60 μm vessel resulting in velocity of 750 μm/s (27 frames stacked with 30 fps; ie, unmodified MSC remains in the field of view for $<$ 0.9 seconds). Bar represents 50 μm.

(1) covalent biotinylation of the cell surface through the reaction of cell surface amine groups with *N*-hydroxy-succinimide functionalities, (2) functionalization of the biotin with streptavidin, and (3) attachment of a nanometer-scale polymer construct containing biotinylated sLe^x (Figure 1A). The covalent functionalization of MSC resulted in successful immobilization of biotin and streptavidin on the MSC surface that was subsequently used to immobilize sLe^x on the MSC surface. The covalent conjugation of biotin on the MSC surface was characterized by the fluorescence signal of rhodamine-streptavidin (SR) attached to the biotin after BNHS and SR treatment (day 0) and after 7 days after BNHS and SR treatment (supplemental Figure 2). The temporal stability and accessibility of the covalently conjugated biotin on the MSC surface were examined by quantifying the fluorescence signal of SR added to the cells at different time points, which indicated that covalent immobilization of biotin with BNHS treatment resulted in a stable and accessible biotin on the cell surface up to 7 days (supplemental Figure 3). The relatively sustained fluorescence intensity from rhodamine-conjugated streptavidin up to day 7 may indicate an excess of biotin on the cell surface; as cells proliferated, the surface concentration of biotin remained higher than what was required to saturate the streptavidin, a much larger molecule compared with biotin. To maximize the sLe^x density on the MSC surface, the efficiency of conjugation for all 3 steps was optimized with flow cytometric analysis (supplemental Figure 1). The optimized condition resulted in 10, 1, and 5 minutes of reaction time for steps 1, 2, and 3, respectively, for the cell surface modification (Figure 1A).Under the optimized condition, the sLe^x density on MSC surface, determined with purified HECA-452 and the secondary antibody (FITC mouse anti–rat IgM), was approximately 38.5 $\pm$ 19.5 sLe^x moieties/μm^2 (ie, $\sim$ 27 500 $\pm$ 13 600 sLe^x ligands per cell), whereas the site density of sLe^x on neutrophils is approximately 400 sLe^x moieties/μm^2, resulting in approximately 90 700 sLe^x ligands on the cell surface.[26]

Cell surface modification has minimal impact on MSC phenotype

Importantly, the methods used to engineer cell homing did not impact the phenotype of the MSCs. The results demonstrate that covalent immobilization of sLe^x on the MSC surface has minimal impact on the cells. Specifically, the covalent immobilization of sLe^x through biotin-streptavidin did not affect the viability, kinetics of adhesion to tissue culture plastic, proliferation, and multilineage differentiation potential (supplemental Figure 4). The role of MSC-secreted paracrine factors is important for providing immunomodulatory function and for maintaining the cellular microenvironment of tissues,[27] which does not appear to be compromised in cells that have been modified with sLe^x. Specifically, the secretion of paracrine factors by the MSCs was examined by quantifying SDF-1, IGF-1, and PGE2 secretion in the culture media using ELISA assays, and no significant difference was observed between the levels of expression of the paracrine factors for the MSCs modified with sLe^x compared with the PBS-treated cells (supplemental Figure 5). A temporary reduction in the expression of MSC markers CD90, CD29, and a homing receptor CD49d on the MSC surface was observed immediately after sLe^x modification by flow cytometry analysis (supplemental Figure 5). The reduced antibody binding indicates that these surface proteins are altered through the chemical modification or that the accessibility of the surface antigens to antibodies is restricted. The recovery of the surface antigens after 24 hours indicates that the reduced binding is only temporary.

sLe^x-modified MSCs roll on P-selectin substrate in vitro

The dynamic adhesive interactions between immobilized sLe^x on the MSC surface and P-selectin were characterized with an in vitro flow chamber assay. The enhanced interaction of sLe^x-modified MSCs was evident from the lower velocity and increased number of interacting cells compared with unmodified MSCs. The chemically immobilized sLe^x reduced the velocity of MSCs on P-selectin substrates from approximately 74 $\pm$ 15 μm/s to approximately 0.5 $\pm$ 0.3 μm/s at a wall shear stress of 0.36 dyne/cm^2 ($P < .001$, Figure 1B). The number of interacting cells (ie, rolling or firmly adherent cells on the surface within a 0.45-mm^2 surface area in a 10-second interval) increased from 20 cells/mm^2 for PBS-treated MSCs to 150 cells/mm^2 for sLe^x-modified MSCs ($P < .05$, Figure 1C). This indicates that MSCs engineered with sLe^x interact with P-selectin through increased adhesive interactions. To examine the

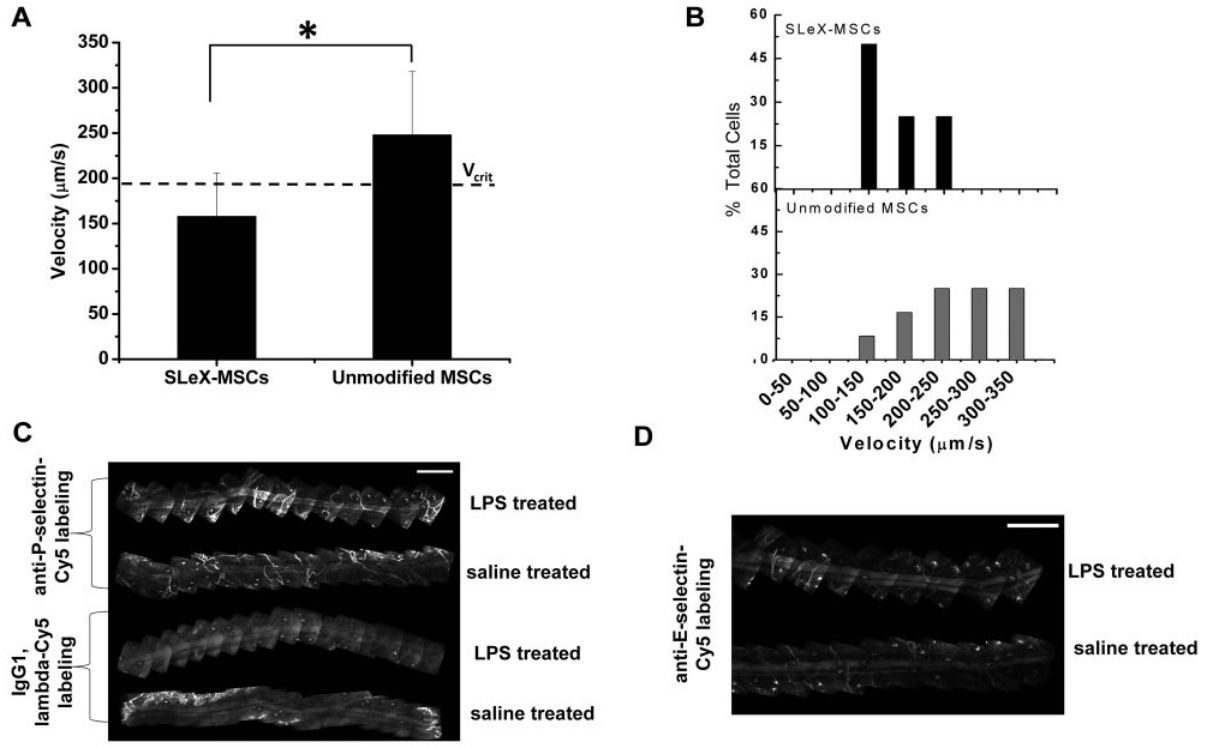

Figure 3. In vivo rolling velocity of surface engineering MSCs and selectin expression. (A) Velocity of sLe^x-modified MSCs and unmodified MSCs on inflamed endothelium within a vessel of 47 μm diameter where the critical velocity (V_{crit}) is 191 μm/s. (B) Representative distribution of velocity showing 75% of sLe^x-MSCs and 25% of unmodified MSCs are below the critical velocity. Cells traveling below the critical velocity decelerate on the vessel wall through receptor/ligand-mediated adhesive interactions. (C) In vivo confocal images of anti–P-selectin–labeled postcapillary venules 24 hours after LPS stimulation. Top: Two venules represent anti–P-selectin–Cy5 labeling in LPS-treated ear and saline-treated ear. Bottom: Two venules represent IgG1, λ-Cy5 labeling in LPS-treated ear and saline-treated ear. Bar represents 500 μm. (D) In vivo confocal images of anti–E-selectin–labeled postcapillary venules 24 hours after LPS stimulation. Top venule represents anti–E-selectin–Cy3 labeling in LPS-treated ear, and bottom venule represents anti–E-selectin–Cy3 labeling in saline-treated ear. Bar represents 500 μm *$P < .05$.

specificity of sLe^x as a rolling ligand, a nonrolling ligand, biotinylated monosaccharide (glucose), was immobilized on the MSC surface (instead of sLe^x). The velocity of glucose-modified MSCs (Figure 1B) was substantially higher than sLe^x-MSCs, and significantly fewer glucose-modified MSCs (Figure 1C) interacted with P-selectin compared with sLe^x-MSCs. As the shear stress was increased from 0.36 dyne/cm^2 to 1.89 dyne/cm^2, the velocity of the sLe^x-modified cells increased modestly from 0.5 μm/s to 2 μm/s (Figure 1D). Remarkably, the cell rolling response of sLe^x-modified MSCs was similar to the rolling response of HL60 cells[28] (a model cell line used to examine cell rolling on selectin-coated substrates in vitro) up to a shear stress of approximately 2 dyne/cm^2. In addition, the number of sLe^x-MSCs interacting with P-selectin surface remains relatively constant up to approximately 2 dyne/cm^2 (supplemental Figure 6). Thus, the sLe^x-modified MSCs induced a rolling response through promoting specific interactions with P-selectin by mimicking P-selectin–mediated leukocyte rolling.

sLe^x-modified MSCs roll on inflamed endothelium in vivo

After demonstrating enhanced rolling interactions in vitro, we examined the rolling of the engineered MSCs on activated endothelium in vivo with dynamic real-time intravital confocal microscopy using injection of LPS into the ear of a mouse as the model for inflammation. sLe^x-modified and unmodified MSCs were pretreated with tracker dyes infused via the tail vein simultaneously. To avoid potential bias for imaging, the type of dye used to stain the sLe^x-modified and unmodified MSCs was alternated between experiments. The rolling interactions of the MSCs were analyzed within the first hour after infusion of cells. The velocity of the sLe^x-modified MSCs and unmodified MSCs that interacted with the venular endothelium was determined within the same field of view to minimize the differences because of flow conditions, the level of inflammation, and differences in imaging. The interaction of sLe^x-modified MSCs with the inflamed endothelium induced the cells to roll with a reduced velocity compared with the unmodified MSCs along the vessel surface (Figure 2A-B). Figure 2C-D shows representative time-lapsed images showing sLe^x-modified MSCs rolling along the inflamed endothelium while unmodified MSCs did not exhibit any interactions. The reduced velocity of sLe^x-modified MSCs on the activated endothelium indicates enhanced interaction with the vessel wall and is characteristic of cell rolling observed in vivo. This demonstrates that MSCs engineered with sLe^x were able to interact with the endothelium in vivo and thus signifies the importance of cell membrane modification to induce a rolling response. Rolling interactions in vivo were analyzed using a standard critical velocity calculation, which represents the lowest velocity at which a cell traveling close to the vessel wall can move without specific receptor/ligand-mediated adhesive interactions.[22,28] For example, the critical velocity for a vessel with a 47-μm diameter was 191 μm/s. The average velocity of the sLe^x-modified MSCs along the activated endothelium of the vessel was 158 ± 48 μm/s compared with unmodified MSCs which had an average velocity of 247 ± 70 μm/s (Figure 3A, $P < 0.05$). Thus MSCs engineered with sLe^x were classified as rolling, whereas unmodified cells traveled at a significantly higher velocity. In addition, the

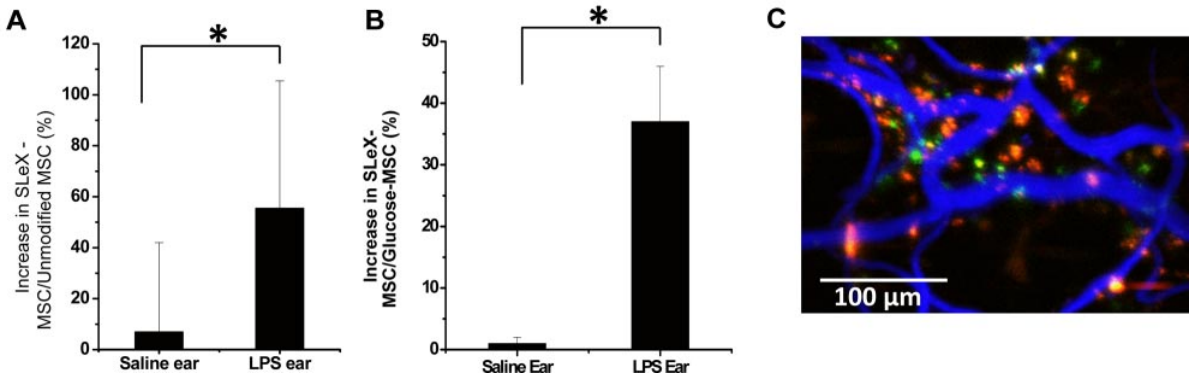

Figure 4. Targeted homing of surface engineering MSCs to inflamed tissue. (A) Percentage increase in sLe^x-modified MSCs compared with unmodified MSCs that homed to the inflamed and saline ear (noninflamed) 24 hours after systemic infusion. The average number of sLe^x-modified MSCs (per field of view) that homed to the inflamed ear was 48 compared with 31 unmodified MSCs, whereas the average number of sLe^x-modified MSCs (per field of view) that homed to the saline ear (noninflamed) was 31 compared with 29 unmodified MSCs. (B) Representative image of MSC localization in the inflamed ear at 24 hours after injection of DiD-labeled sLe^x-MSCs (red) and DiR-labeled unmodified MSCs (green). Most cells extravasated though the vessel walls (visualized by FITC-dextran, blue). No differences in extravasation efficiency were observed, thus indicating that the enhanced homing was because of an engineered rolling response through MSC surface functionalization with sLe^x *$P < .05$.

distribution of velocities of the cells (Figure 3B) shows that 75% of sLe^x-MSCs in the field of view that were interacting with the vessel wall within inflamed tissue were rolling, whereas only 25% of the unmodified MSCs were rolling. The wall shear stress for the 47-μm-diameter vessel was approximately 8 dyne/cm^2. To examine the specificity of the interactions between the sLe^x and selectins, the rolling interactions were examined with MSCs modified with a nonrolling ligand, glucose. Compared with glucose-modified MSCs, sLe^x-modified MSCs exhibited enhanced interaction with the inflamed endothelium. This indicates that the enhanced interaction of sLe^x-MSCs is the result of the specific interactions between the sLe^x immobilized on the MSC surface and the selectins expressed on the activated endothelium. Specifically, the average velocity of the glucose-modified MSCs was significantly higher than sLe^x-MSCs (average glucose-MSC velocity, 748 ± 217 μm/s; and average sLe^x-MSCs velocity, 529 ± 226 μm/s, $P < 0.0001$; within a 60-μm-diameter vessel with a critical velocity of 571 μm/s and wall shear stress ~ 17 dyne/cm^2), and the distribution of the velocities of the cells shows only 23% glucose-modified MSCs were rolling compared with 63% of sLe^x-MSCs on the activated endothelium (supplemental Figure 7A-B). Under inflamed conditions, 50% of leukocytes have been shown to roll with a velocity 60 ± 36 μm/s[29] under shear stress of 8 dyne/cm^2, and specifically 40% of neutrophils have been shown in a separate study to roll on a 31-μm-diameter vessel with a velocity 151 ± 10 μm/s.[28] Thus, the immobilized sLe^x on the surface of the MSCs specifically induced rolling interactions on the inflamed endothelium compared with unmodified MSCs. Because MSCs exhibit reduced expression of key homing ligands during culture expansion that contributes to their inefficient homing potential,[10] our results signify the importance of engineering the MSC surface with rolling ligands to reduce the velocity of cells in the bloodstream within sites of inflammation. These results also indicate that sLe^x-modified MSCs are able to induce adhesive interactions with inflamed endothelium at high shear stress (up to 17 dyne/cm^2) and in large blood vessels. This is probably in part the result of the extension of the sLe^x moieties from the MSC surface, which is estimated to be approximately 43 nm (the length of the multivalent sLe^x polymeric construct is estimated to be 30 nm,[30] the globular dimension of streptavidin diameter is ~ 11 nm, and the BNHS sulfonated biotin with spacer is ~ 2.2 nm). Thus, the extension of sLe^x moieties from the MSC surface is close to the 60-nm reported length of PSGL-1 on the surface of neutrophils that is required to bypass the formidable source of steric and electrostatic repulsion provided by the endothelial cell glycocalyx.[31]

It is important to consider that rolling interactions in vivo are typically highly variable and generally depend on the vessel type and dimension, velocity of blood flow and wall shear stress, level of inflammation, and particular animal model. Importantly, the rolling velocity of sLe^x-modified MSCs closely resembled that of leukocytes and was mediated through specific interactions between the chemically immobilized sLe^x on the MSC surface and selectins within vessels in inflamed tissue. To verify that P-selectin was up-regulated after LPS treatment, in vivo immunolabeling was performed on inflamed and saline-treated ears 24 hours after LPS stimulation. A total of 3- or 4-mm of postcapillary venules were imaged for both anti–P-selectin and the isotype control (Figure 3C). The LPS-treated anti–P-selectin–labeled venule showed increased fluorescence signal compared with anti–P-selectin–labeled saline-treated venules and isotype-labeled venules. Although E-selectin has been shown to be up-regulated on endothelium 4 days after intraperitoneal administration of 50 μg LPS and within 4 hours after injecting 20 μg LPS in the footpad of rodents,[32,33] E-selectin up-regulation was not observed in the present study (Figure 3D).

sLe^x modification facilitates MSC homing to inflamed tissue

To determine whether the engineered rolling response could be used to increase the homing of systemically administered MSCs to inflamed tissue, we examined the total number of cells, both sLe^x-modified MSCs and unmodified MSCs, that homed to the inflamed (LPS) ear 24 hours after infusion. Figure 4A shows that sLe^x-modified MSCs localized to the inflamed ear with 56% increased efficiency compared with the unmodified MSCs, whereas no significant difference was observed between the numbers of sLe^x-MSCs and unmodified MSCs within the noninflamed (saline) ear. The enhanced homing of sLe^x-MSCs to inflamed tissue compared with unmodified MSCs shows the significance of the engineered adhesion ligands to improve homing of the cells. Furthermore, no difference in homing of the sLe^x-MSCs and unmodified MSCs within the noninflamed ear signifies the role of the immobilized sLe^x as homing ligand. It is also important to consider that the sLe^x modification did not impact homing to the

noninflamed ear, suggesting that the modification process did not compromise the native homing ligands on the MSC surface. Noninflamed endothelium of mouse ear vessels constitutively express selectins,[32,34] which probably contributed to the basal levels of homing observed for both the unmodified MSCs and sLe^x-MSCs within the noninflamed ear. On investigation of the specificity of sLe^x interactions with selectins within the inflamed ear, we observed that homing of sLe^x-MSCs was significantly more efficient than the glucose-modified MSCs and homing of the glucose-modified MSCs showed a similar response to the unmodified MSCs (supplemental Figure 7C). In addition, treatment with blocking antibody against P-selectin resulted in a 25% reduction of the homing of sLe^x-MSCs to the inflamed ear compared with the isotype control ($P < .05$). Specifically, the average number of sLe^x-MSCs (per the field of view) dropped from approximately 30 in the isotope control to approximately 23 after blocking P-selectin in the inflamed ear. This partial but significant decrease of the homing of sLe^x-MSCs to the inflamed ear further confirms the specific role of the P-selectin in mediating the homing response of sLe^x-modified MSCs. These results indicate that enhanced homing efficiency for sLe^x-MSCs was mediated in part by rolling interactions between selectin and sLe^x. However, the incomplete response to the anti–P-selectin treatment also suggests that, in addition to P-selectin, homing sLe^x-MSCs to the inflamed ear is also mediated by other receptors expressed by the inflamed endothelium. Figure 4B shows increased number of sLe^x-MSCs (red) homed to the inflamed ear compared with unmodified MSCs (green). To ensure efficient homing, it is critical for the MSCs to extravasate through the endothelium into the tissue. The majority ($> 90\%$) of sLe^x-MSCs localized within the inflamed tissues had extravasated from the blood vessels after 24 hours, indicating that the ability of the MSCs to transmigrate through the endothelium was not affected by the covalent modification of the cell surface with sLe^x. In addition, no significant difference was observed in the extravasation efficiency between the sLe^x-MSCs ($88\% \pm 11\%$) and unmodified MSCs ($83\% \pm 19\%$) in the noninflamed ear. The increased homing response is probably critical for improving the engraftment of MSCs, within diseased tissues after systemic injection, leading to improved therapeutic outcome. The proof of principle for this hypothesis is provided by approaches that have involved enzymatic and genetic modifications of cells to overexpress adhesion or chemokine receptors, leading to improved homing and functional outcome in animal models.[7,17,35]

The success of MSC systemic therapy is limited by poor homing efficiency.[10] This study demonstrates that chemical modification of primary human MSCs under controlled conditions can promote a robust rolling response in vivo leading to increased homing to inflamed tissue. Most significantly, it is demonstrated that inducing a rolling response is critical to increase the homing of systemically delivered MSCs. We have shown that the conditions that maximize cell rolling preserve the MSC phenotype, including their multilineage differentiation potential and their ability to secrete paracrine factors. Although the modification with sLe^x increased homing of MSCs to a site of inflammation, we do not anticipate that this will directly reduce entrapment of MSCs in the microvascular of organs, such as the lungs. These results provide a roadmap for introducing functional adhesion ligands on the surface of cells to promote a robust homing response. This method offers a simple approach to explore engineered cell homing and potentially target any cell type to specific tissues via the circulation.

Acknowledgments

This work was supported by the American Heart Association (grant 0970178N) and the National Institutes of Health (grants DE019191, HL095722, and HL097172, J.M.K.) as well as the Massachusetts Institute of Technology Undergraduate Research Opportunities Program. P.K.V. was supported by Kauffman Foundation Entrepreneur (Postdoctoral Fellowship). W.Z. was supported by the Human Frontier Science Program (Postdoctoral Fellowship).

Authorship

Contribution: D.S., J.A.S., C.P.L., and J.M.K. designed the research and the experiments; D.S., S.S., J.A.S., J.A.P., and D.P.S. performed the experiments; D.S., J.A.S., J.A.P., L.J.M., S.K., W.Z., P.K.V., R.S., C.P.L., R.K., and J.M.K. analyzed the data; and D.S., J.A.S., C.P.L., R.K., and J.M.K. wrote the manuscript and contributed to the interpretation of the results.

Conflict-of-interest disclosure: J.M.K. is a co-owner of Megacell Therapeutics, a company that has an option to license IP generated by J.M.K. J.M.K. may benefit financially if the IP is licensed and further validated. The interests of J.M.K. were reviewed and are subject to a management plan overseen by the Brigham & Women's Hospital and Partners HealthCare in accordance with their conflict of interest policies. The remaining authors declare no competing financial interests.

Correspondence: Jeffrey M. Karp, Center for Regenerative Therapeutics & Department of Medicine, Brigham & Women's Hospital, Harvard Medical School, Harvard Stem Cell Institute, Harvard–Massachusetts Institute of Technology, Division of Health Sciences and Technology, 65 Landsdowne St, Cambridge, MA 02139; e-mail: jkarp@rics.bwh.harvard.edu.

References

1. Ankrum J, Karp JM. Mesenchymal stem cell therapy: two steps forward, one step back. *Trends Mol Med.* 2010;16(5):203-209.
2. Tuan RS, Boland G, Tuli R. Adult mesenchymal stem cells and cell-based tissue engineering. *Arthritis Res Ther.* 2003;5(1):32-45.
3. Bianco P, Riminucci M, Gronthos S, Robey PG. Bone marrow stromal stem cells: nature, biology, and potential applications. *Stem Cells.* 2001; 19(3):180-192.
4. Phinney DG, Prockop DJ. Concise review. Mesenchymal stem/multipotent stromal cells: the state of transdifferentiation and modes of tissue repair—current views. *Stem Cells.* 2007;25(11): 2896-2902.
5. Zhang M, Mal N, Kiedrowski M, et al. SDF-1 expression by mesenchymal stem cells results in trophic support of cardiac myocytes after myocardial infarction. *FASEB J.* 2007;21(12):3197-3207.
6. Barbash IM, Chouraqui P, Baron J, et al. Systemic delivery of bone marrow-derived mesenchymal stem cells to the infarcted myocardium: feasibility, cell migration, and body distribution. *Circulation.* 2003;108(7):863-868.
7. Sackstein R, Merzaban JS, Cain DW, et al. Ex vivo glycan engineering of CD44 programs human multipotent mesenchymal stromal cell trafficking to bone. *Nat Med.* 2008;14(2):181-187.
8. Wynn RF, Hart CA, Corradi-Perini C, et al. A small proportion of mesenchymal stem cells strongly expresses functionally active CXCR4 receptor capable of promoting migration to bone marrow. *Blood.* 2004;104(9):2643-2645.
9. Rombouts WJC, Ploemacher RE. Primary murine MSC show highly efficient homing to the bone marrow but lose homing ability following culture. *Leukemia.* 2003;17(1):160-170.
10. Karp JM, Leng Teo GS. Mesenchymal stem cell homing: the devil is in the details. *Cell Stem Cell.* 2009;4(3):206-216.
11. Granger DN, Kubes P. The microcirculation and inflammation: modulation of leukocyte-endothelial cell adhesion. *J Leukoc Biol.* 1994;55(5):662-675.
12. Luster AD, Alon R, von Andrian UH. Immune cell migration in inflammation: present and future

therapeutic targets. *Nat Immunol.* 2005;6(12):1182-1190.

13. Sackstein R. The bone marrow is akin to skin: HCELL and the biology of hematopoietic stem cell homing. *J Invest Dermatol.* 2004;122(5):1061-1069.
14. Simon SI, Green CE. Molecular mechanics and dynamics of leukocyte recruitment during inflammation. *Annu Rev Biomed Eng.* 2005;7:151-185.
15. Eniola AO, Willcox PJ, Hammer DA. Interplay between rolling and firm adhesion elucidated with a cell-free system engineered with two distinct receptor-ligand pairs. *Biophys J.* 2003;85(4):2720-2731.
16. Jung U, Norman KE, Scharffetter-Kochanek K, Beaudet AL, Ley K. Transit time of leukocytes rolling through venules controls cytokine-induced inflammatory cell recruitment in vivo. *J Clin Invest.* 1998;102(8):1526-1533.
17. Cheng Z, Ou L, Zhou X, et al. Targeted migration of mesenchymal stem cells modified with CXCR4 gene to infarcted myocardium improves cardiac performance. *Mol Ther.* 2008;16(3):571-579.
18. Sarkar D, Vemula PK, Teo GS, et al. Chemical engineering of mesenchymal stem cells to induce a cell rolling response. *Bioconjug Chem.* 2008;19(11):2105-2109.
19. Sarkar D, Vemula PK, Zhao W, Gupta A, Karnik R, Karp JM. Engineered mesenchymal stem cells with self-assembled vesicles for systemic cell targeting. *Biomaterials.* 2010;31(19):5266-5274.
20. Veilleux I, Spencer JA, Biss DP, Côté D, Lin CP. In vivo cell tracking with video rate multimodality laser scanning microscopy. *IEEE J Sel Top Quantum Electron.* 2008;14:10-18.
21. Ismail T, Howl J, Wheatley M, McMaster P, Neuberger JM, Strain AJ. Growth of normal human hepatocytes in primary culture: effect of hormones and growth factors on DNA synthesis. *Hepatology.* 1991;14(6):1076-1082.
22. Sperandio M, Pickard J, Unnikrishnan S, Acton ST, Ley K. Analysis of leukocyte rolling in vivo and in vitro. *Methods Enzymol.* 2006;416:346-371.
23. Long DS, Smith ML, Pries AR, Ley K, Damiano ER. Microviscometry reveals reduced blood viscosity and altered shear rate and shear stress profiles in microvessels after hemodilution. *Proc Natl Acad Sci U S A.* 2004;101(27):10060-10065.
24. Smith ML, Long DS, Damiano ER, Ley K. Near-wall micro-PIV reveals a hydrodynamically relevant endothelial surface layer in venules in vivo. *Biophys J.* 2003;85(1):637-645.
25. Lipowsky HH, Usami S, Chien S. In vivo measurements of "apparent viscosity" and microvessel hematocrit in the mesentery of the cat. *Microvasc Res.* 1980;19(3):297-319.
26. Rodgers SD, Camphausen RT, Hammer DA. Sialyl Lewis(x)-mediated, PSGL-1-independent rolling adhesion on P-selectin. *Biophys J.* 2000;79(2):694-706.
27. Caplan AI. Adult mesenchymal stem cells for tissue engineering versus regenerative medicine. *J Cell Physiol.* 2007;213(2):341-347.
28. Norman KE, Moore KL, McEver RP, Ley K. Leukocyte rolling in vivo is mediated by P-selectin glycoprotein ligand-1. *Blood.* 1995;86(12):4417-4421.
29. Maly P, Thall A, Petryniak B, et al. The alpha(1,3)fucosyltransferase Fuc-TVII controls leukocyte trafficking through an essential role in L-, E-, and P-selectin ligand biosynthesis. *Cell.* 1996;86(4):643-653.
30. Zou X, Shinde Patil VR, Dagia NM, et al. PSGL-1 derived from human neutrophils is a high-efficiency ligand for endothelium-expressed E-selectin under flow. *Am J Physiol Cell Physiol.* 2005;289(2):C415-C424.
31. Patel KD, Nollert MU, McEver RP. P-selectin must extend a sufficient length from the plasma membrane to mediate rolling of neutrophils. *J Cell Biol.* 1995;131(6):1893-1902.
32. Runnels JM, Zamiri P, Spencer JA, et al. Imaging molecular expression on vascular endothelial cells by in vivo immunofluorescence microscopy. *Mol Imaging.* 2006;5(1):31-40.
33. Henseleit U, Steinbrink K, Goebeler M, et al. E-selectin expression in experimental models of inflammation in mice. *J Pathol.* 1996;180(3):317-325.
34. Weninger W, Ulfman LH, Cheng G, et al. Specialized contributions by alpha(1,3)-fucosyltransferase-IV and FucT-VII during leukocyte rolling in dermal microvessels. *Immunity.* 2000;12(6):665-676.
35. Zhang D, Fan GC, Zhou X, et al. Over-expression of CXCR4 on mesenchymal stem cells augments myoangiogenesis in the infarcted myocardium. *J Mol Cell Cardiol.* 2008;44(2):281-292.